Polysaccharide Compositions of Intervessel Pit Membranes Contribute to Pierce's Disease Resistance of Grapevines[1][OA]

Qiang Sun*, L. Carl Greve, and John M. Labavitch

Department of Biology, University of Wisconsin, Stevens Point, Wisconsin 54481 (Q.S.); and
Department of Plant Sciences, University of California, Davis, California 95616 (L.C.G., J.M.L.)

Symptom development of Pierce's disease (PD) in grapevine (*Vitis vinifera*) depends largely on the ability of the bacterium *Xylella fastidiosa* to use cell wall-degrading enzymes (CWDEs) to break up intervessel pit membranes (PMs) and spread through the vessel system. In this study, an immunohistochemical technique was developed to analyze pectic and hemicellulosic polysaccharides of intervessel PMs. Our results indicate that PMs of grapevine genotypes with different PD resistance differed in the composition and structure of homogalacturonans (HGs) and xyloglucans (XyGs), the potential targets of the pathogen's CWDEs. The PMs of PD-resistant grapevine genotypes lacked fucosylated XyGs and weakly methylesterified HGs (ME-HGs), and contained a small amount of heavily ME-HGs. In contrast, PMs of PD-susceptible genotypes all had substantial amounts of fucosylated XyGs and weakly ME-HGs, but lacked heavily ME-HGs. The intervessel PM integrity and the pathogen's distribution in *Xylella*-infected grapevines also showed differences among the genotypes. In pathogen-inoculated, PD-resistant genotypes PM integrity was well maintained and *Xylella* cells were only found close to the inoculation site. However, in inoculated PD-susceptible genotypes, PMs in the vessels associated with bacteria lost their integrity and the systemic presence of the *X. fastidiosa* pathogen was confirmed. Our analysis also provided a relatively clear understanding of the process by which intervessel PMs are degraded. All of these observations support the conclusion that weakly ME-HGs and fucosylated XyGs are substrates of the pathogen's CWDEs and their presence in or absence from PMs may contribute to grapevine's PD susceptibility.

Plant vascular diseases (e.g. Pierce's disease [PD] of grapevines [*Vitis vinifera*], Dutch elm disease, oak [*Quercus* spp.] wilt, and *Fusarium* wilt in cotton [*Gossypium hirsutum*] and tomato [*Solanum lycopersicum*]) are among the most devastating diseases of crop and forest plants, causing tremendous economic losses and environmental concerns (Tattar, 1989). The first crucial step in disease symptom development for most vascular diseases is the spread of the initially introduced, small pathogen population away from the site where it was placed in the host plant by a vector. Thus, vascular system-localized features of a potential host plant will play an important role in determining whether the few pathogen cells that have been introduced will spread systemically, causing disease, or remain local and have no lasting impact on the infected plant. PD of grapevines is currently jeopardizing the wine and table grape industries in the United States because of the relatively recent arrival of the glassy-winged sharpshooter (*Homalodisca vitripennis*), a particularly effective vector of *Xylella fastidiosa*, the bacterium that causes PD (Varela et al., 2001). *X. fastidiosa* is a xylem-limited bacterium that spreads only through the vessel system of a host grapevine (Purcell and Hopkins, 1996), thus, any factors affecting the systemic expansion of the bacterium population that has been introduced initially into one or very few vessels should be relevant to the resistance versus susceptibility of the infected vine.

Because it is the only avenue for the pathogen's spread, the vessel system of grapevine has attracted a lot of research attention (e.g. Hopkins and Mollenhauer, 1975; Chatelet et al., 2006; Sun et al., 2006, 2007; Thorne et al., 2006). Each vessel in a grapevine's secondary xylem is composed of a few vessel elements differentiated from elongated fusiform initials that were axially arranged end to end. The vessel elements of a vessel have simple perforations at their ends except at the uppermost and lowermost ends of the vessel, allowing free movement of water and solutes from one

[1] This work was supported by the Pierce's Disease Control Program and the Glassy-Winged Sharpshooter Board of the California Department of Food and Agriculture (California Department of Food and Agriculture contract no. 08–0174 to J.M.L and Q.S.) and the U.S. Department of Agriculture-University of California Pierce's Disease Grants Program (U.S. Department of Agriculture National Institute of Food and Agriculture contract no. 2010–266 to Q.S. and J.M.L).

* Corresponding author; e-mail qsun@uwsp.edu.

The author responsible for distribution of materials integral to the findings presented in this article in accordance with the policy described in the Instructions for Authors (www.plantphysiol.org) is: Qiang Sun (qsun@uwsp.edu).

[OA] Open Access articles can be viewed online without a subscription.

www.plantphysiol.org/cgi/doi/10.1104/pp.110.168807

end of the vessel to the other. However, the individual vessels are relatively short (average length of 3–4 cm [Thorne et al., 2006] with an occasional quite long vessel), thus systemic movement of water, minerals, or bacteria requires passage through multiple adjacently interconnected vessels.

Movement from one vessel to the next requires passage through pit pairs, specialized wall structures that connect a vessel to its neighbors. In grapevines, contact with neighboring vessels occurs at multiple locations along the vessel's length and scalariform (i.e. organized in a ladder-like pattern) pit pairs always occur in the wall regions where two adjacent vessels are in contact (Sun et al., 2006). An intervessel pit pair includes two opposing pits, one perforating the thick secondary wall of each of the neighboring vessels. Since no secondary cell walls are deposited in the wall region where pit pairs develop, adjacent vessels at each pit pair are separated only by two thin primary cell walls and one middle lamella. This assemblage is collectively called a pit membrane (PM; Esau, 1977; Evert, 2006). In terms of intervessel PM porosity (i.e. the spaces between the polysaccharides of the PM's primary walls and middle lamella that might allow free passage of particles), pores of up to several hundred nanometers have been observed in very few cases (Sperry et al., 1991; Fleischer et al., 1999) and pore sizes of grapevine PMs have been reported to vary between 5 and 20 nm (Choat et al., 2003; Pérez-Donoso et al., 2010). This somewhat tortuous path along the length of a stem provides some resistance to water movement. However, the passage of *X. fastidiosa* cells (0.25–0.5 μm $\times$ 1–4 μm in size; Mollenhauer and Hopkins, 1974) should be prevented by the small pore sizes of the intervessel PMs, as long as the PMs remain intact.

It has been proposed that *X. fastidiosa* cells use cell wall-degrading enzymes (CWDEs) to digest PM polysaccharides and achieve their systemic spread, just as other fungal and bacterial pathogens do (Barras et al., 1994; Newman et al., 2004). Microscopic examination of infected grapevines has shown *X. fastidiosa* cells traversing intervessel PMs (Newman et al., 2003; Ellis et al., 2010). *X. fastidiosa*'s genome contains genes whose sequences suggest that they encode two types of CWDEs: Polygalacturonase (PG) and endo-1,4-β-glucanase (EGase; Simpson et al., 2000) and heterologous expression of the putative *X. fastidiosa* PG and EGase genes (Roper et al., 2007; Pérez-Donoso et al., 2010) produced proteins capable of digesting homogalacturonan pectin (HG) and xyloglucan (XyG), respectively, polysaccharides that are often found in dicot cell walls (Carpita and Gibeaut, 1993). Furthermore, the introduction of PG and EGase to explanted grapevine stems caused breaks in the PM polysaccharide network and permitted *X. fastidiosa* cells to pass through intervessel PMs (Pérez-Donoso et al., 2010).

Although most commercial genotypes of grapevine are susceptible to PD, many wild *Vitis* genotypes and some hybrids of grapevine and wild *Vitis* genotypes have shown strong PD resistance in greenhouse evaluations (Loomis, 1958; Ruel and Walker, 2006). Studies with some PD-resistant vines using PCR have demonstrated that most *X. fastidiosa* cells that have been inoculated into vine stems, remain quite close to the inoculation sites, while bacteria inoculated into PD-susceptible genotypes spread away from inoculation sites (Fry and Milholland, 1990a, 1990b; Krivanek and Walker, 2005). Thus, the relative PD susceptibilities of different grapevine genotypes might be explained by differences in the susceptibilities of their PM polysaccharides to digestion by *X. fastidiosa*'s PG and EGase. The work in this report examines PM polysaccharide compositions using monoclonal antibodies that recognize HG and fucosylated XyG in the intervessel PMs of several PD-resistant and -susceptible grapevine genotypes. It also explores the integrity of the intervessel PMs in infected vines of these genotypes and the PM degradation process in infected, PD-susceptible grapevines.

RESULTS

Immunohistochemical Detection of Some Pectic and Hemicellulosic Polysaccharides in Intervessel PMs

Intervessel pit pairs in the four grapevine genotypes used in this study were bordered pit pairs. They were transversely elongated almost across the entire widths of the contacting wall regions of two adjacent vessels and arranged in a tightly scalariform pattern along the axis of the contacting wall regions (Figs. 1–3). There were no morphological differences in intervessel pit pairs among the genotypes examined in this study. The structural and morphological details of intervessel pits and PMs were described in Sun et al. (2006).

A technique for immunolocalizing cell wall polysaccharides has been reported by Willats et al. (2002). Our study has combined that technique with confocal laser-scanning microscopy (CLSM) to visualize pectic and hemicellulosic polysaccharides in intervessel PMs of grapevines. The most crucial step in development of our analysis method was identification of the optimal concentration/concentration ranges for use of each of the primary-secondary antibody pairs to detect different polysaccharides in intervessel PMs. To effectively detect a specific polysaccharide or polysaccharide group, the concentration of primary antibody was a 10-fold dilution of its rat hybridoma supernatant (JIM5), a 10- or 50-fold dilution of the rat hybridoma supernatant (JIM7), and a 3- or 10-fold dilution of its mouse hybridoma supernatant (CCRC-M1). The concentration/concentration ranges for the secondary antibodies were a 100- or 200-fold dilution of the hybridoma supernatant for the fluorescein isothiocyanate (FITC)-conjugated rabbit antirat antibody and a 200- or 400-fold dilution for the FITC-conjugated goat antimouse antibody. Because different batches of a

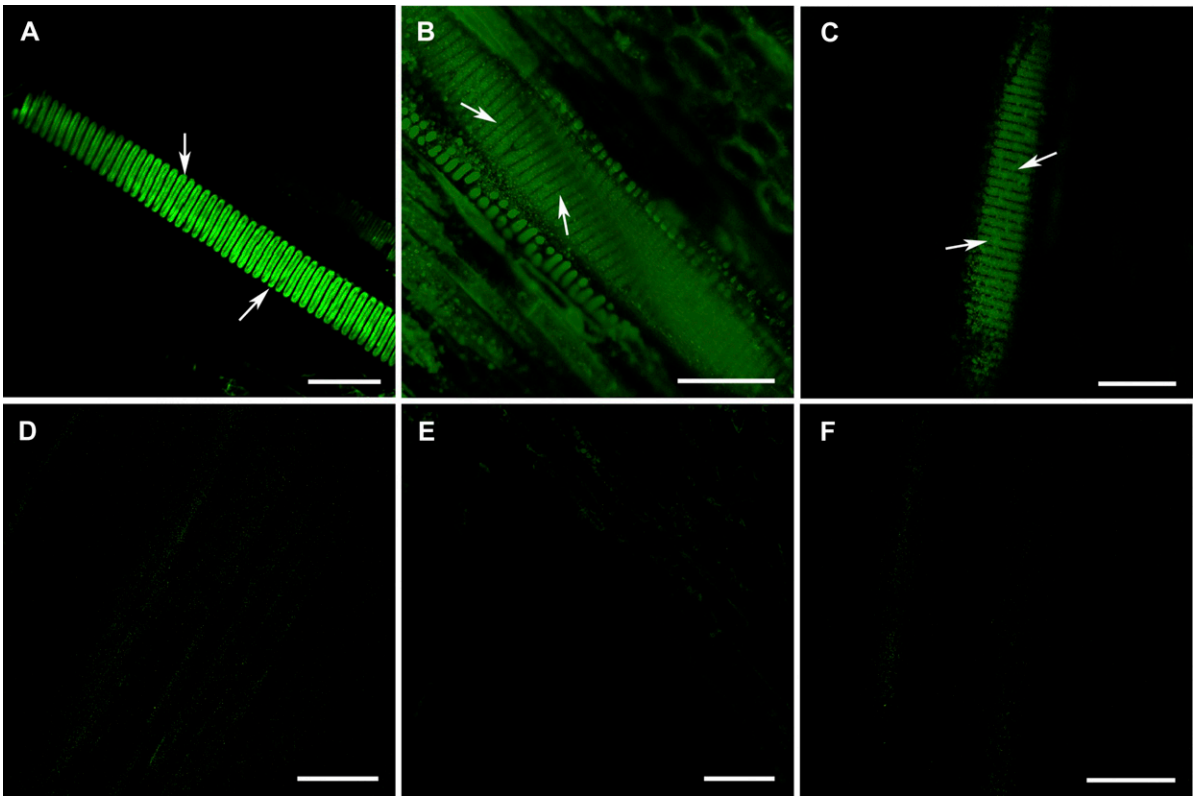

Figure 1. Effectiveness of the immunohistochemical technique with cell wall antibodies and CLSM in detecting some polysaccharide compositions in intervessel PMs from the tangential sectional views of secondary xylem. A to C, Secondary xylem tissue treated with primary antibody and the corresponding secondary antibody. A, Strong fluorescent signal was detected in the intervessel PMs (arrows) of grapevine var. Chardonnay when incubated with CCRC-M1 in a 3-fold dilution of its hybridoma supernatant and FITC-conjugated goat antimouse IgG in a 200-fold dilution. B, Obvious fluorescent signal from the intervessel PMs (arrows) in grapevine var. Riesling incubated with JIM5 and FITC-conjugated rabbit antirat IgG, which were in 10- and 100-fold dilutions, respectively. C, Fluorescence from the intervessel PMs (arrows) in grapevine var. Riesling incubated with JIM7 and FITC-conjugated rabbit antirat IgG, which were in 10- and 100-fold dilutions, respectively. D to F, Secondary xylem tissue of grapevine var. Chardonnay vines in experimental controls, which did not experience the incubation with a primary antibody, a matched secondary antibody, or both. Fluorescent signal was picked up at the same level of amplification as in A to C. D, Xylem tissue not incubated with CCRC-M1 but with FITC-conjugated goat antimouse IgG. No obvious fluorescent signals were detected. E, Xylem tissue incubated with CCRC-M1 but without FITC-conjugated goat antimouse IgG showed no detectable fluorescence. F, No obvious fluorescence from the xylem tissue not incubated with either CCRC-M1 or FITC-conjugated goat antimouse IgG. Bar in each section equals 50 μm.

given hybridoma culture are likely to have different monoclonal antibody (mAb) titers, it may be important to recognize the importance of the determination of appropriate mAb concentrations when working with new mAb preparations and new plant systems. Other modifications including time for sample incubations with primary and secondary antibodies, etc. are indicated in the "Materials and Methods."

The immunohistochemical approach effectively detected two groups of pectic polysaccharides and one group of hemicellulosic polysaccharides in intervessel PMs of grapevine stems. When xylem tissues of each of the four genotypes were treated as described in "Materials and Methods," fucosylated XyGs (Fig. 1A), weakly methyl-esterified HGs (ME-HGs; Fig. 1B), and/or heavily ME-HGs (Fig. 1C) were detected, depending on the genotype examined. There was no or very weak fluorescence from the secondary wall regions of vessels, indicating that interference due to autofluorescence of lignin is not a problem. In control experiments in which xylem tissues were treated without a primary antibody (Fig. 1D), a matched secondary antibody (Fig. 1E), or without both (Fig. 1F), no obvious fluorescence signal was detected from the specimens when the amplification of signals was at the level used in Figure 1, A to C. Thus, the green FITC fluorescence seen in intervessel PMs when matched primary and secondary antibodies are used (Fig. 1, A–C) reflects the presence of the polysaccharide recognized by the primary mAb. These data in each of the controls or treatments for each grapevine genotype were based on an analysis on three vines with three to seven xylem tissue specimens for each vine.

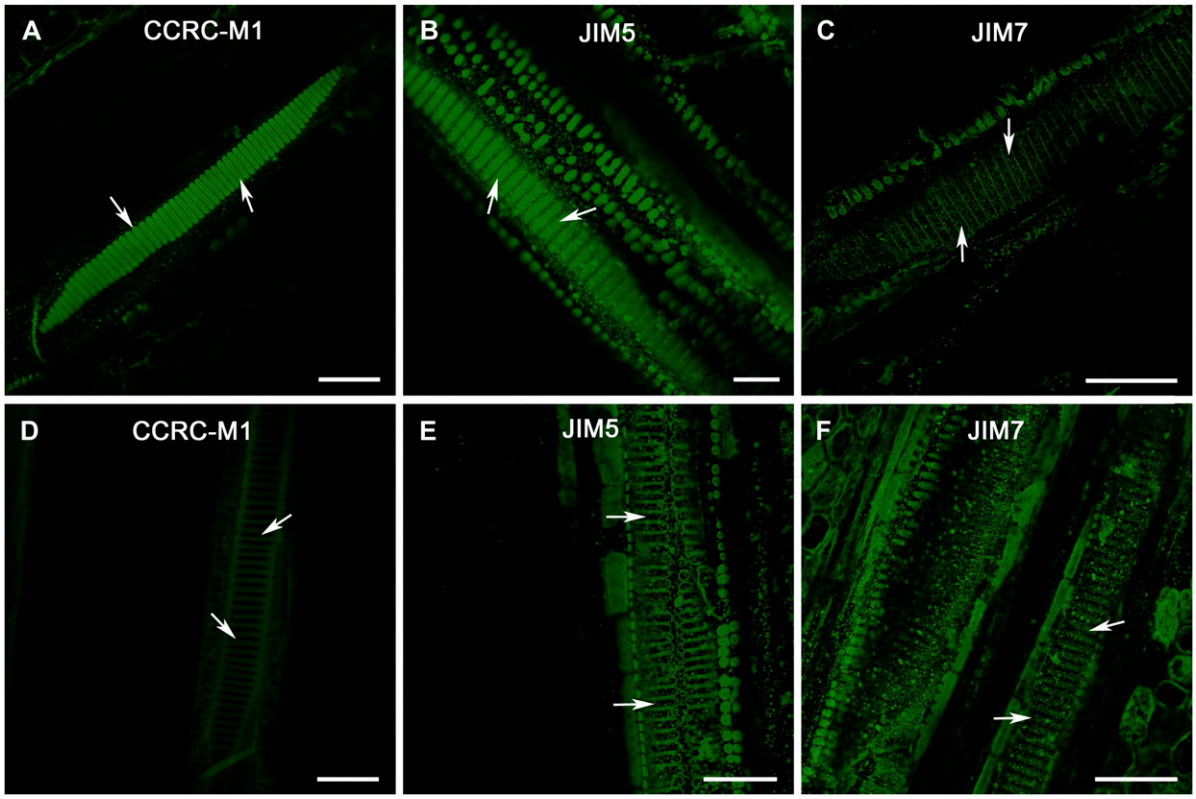

Figure 2. Comparisons of certain pectic and hemicellulosic polysaccharide compositions in intervessel PMs of grapevine genotypes with different PD resistance. A to C, Tangential sectional views of secondary xylem tissue in PD-susceptible grapevine var. Chardonnay vines. D to F, Tangential sectional views of secondary xylem tissue in PD-resistant *V. arizonica X rupestris* (89-0908) vines. A, Strong fluorescent signal from intervessel PMs (arrows) incubated with CCRC-M1. B, Intervessel PMs (arrows) incubated with JIM5 had strong fluorescence. C, No fluorescent signals from intervessel PMs (arrows) incubated with JIM7. D, Signal was considerably amplified relative to that for other sections to pick up very weak autofluorescence to distinguish vessel lateral walls. Even under this condition, fluorescent signal from intervessel PMs (arrows) incubated with CCRC-M1 were below the detectable level. E, Signal was amplified as in D to make vessels' secondary wall regions visible. Even then, there was no detectable fluorescent signal from intervessel PMs (arrows) incubated with JIM5. F, Weak fluorescent signal from intervessel PMs (arrows). Bar in each section equals 50 μm.

Polysaccharide Compositional Differences of Intervessel PMs among Grapevine Genotypes with Differential PD Resistances

The intervessel PM polysaccharides in the four test grapevine genotypes were compared based on their interaction with the primary mAbs and differences between PD-susceptible and -resistant genotypes were detected. Analysis of each genotype with each primary antibody was carried out on three different vines with four to eight xylem tissue segments for each vine. In the PD-susceptible Chardonnay and Riesling genotypes, strong green fluorescence was detected from intervessel PMs in the samples incubated with CCRC-M1 (Fig. 2A) and JIM5 (Fig. 2B), respectively; however there was no obvious fluorescent signal from samples incubated with JIM7 (Fig. 2C). These observations indicated that both fucosylated XyGs and weakly ME-HGs were accessible to the primary and secondary mAbs that recognize these epitopes and were present in the PMs of these PD-susceptible grape genotypes. They also showed that heavily ME-HGs were not present in these PMs or that the epitopes were not accessible to the mAbs used to detect heavily ME-HGs. In the PD-resistant genotypes 89-0908 and U0505-01, a fluorescent signal from intervessel PMs was not detected in tissues incubated with CCRC-M1 (Fig. 2D) and JIM5 (Fig. 2E), respectively, even after the signal (in Fig. 2, D and E) was amplified sufficiently to make visible the lignified vessel secondary walls between PMs, presumably because lignin autofluorescence became apparent with sufficient signal amplification. The fluorescent signal was also weak in tissues treated with JIM7 (Fig. 2F). This indicated that both fucosylated XyGs and weakly ME-HGs are absent from the PMs of these genotypes or that the epitopes recognized by these mAbs may be somehow masked. However, a small amount of heavily ME-HGs was present in these PMs. In brief, fucosylated XyGs and weakly ME-HGs, potentially good substrates for *Xylella*'s PG and EGase, appeared to be not present or inaccessible

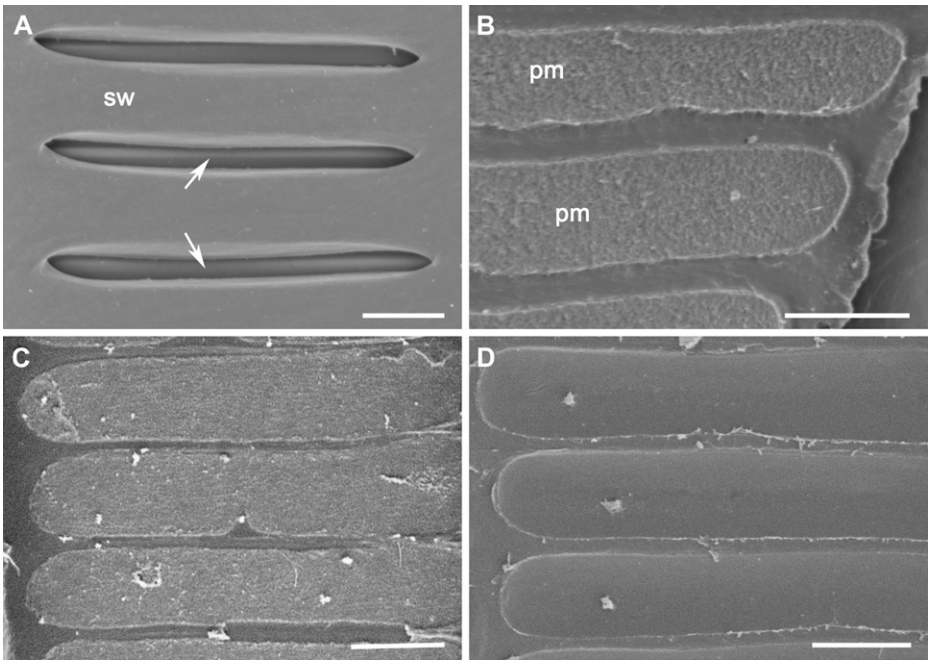

Figure 3. Effect of *Xylella* infection on intervessel PM integrity of PD-susceptible grapevine genotypes (A–C) and PD-resistant grapevine genotype (D). A, Internal surface view of part of a vessel lateral wall in a PBS buffer-inoculated Chardonnay vine. Intervessel pits with secondary cell walls (sw) in place were transversely elongated and arranged scalariformly. Only part of the intervessel PM (arrows) for each pit could be seen through the pit aperture. B to D, The secondary wall borders of each pit were removed to expose the whole intervessel PM. B, Intervessel PMs in a PBS buffer-inoculated Chardonnay vine. C, Intervessel PMs in a vessel not associated with the bacteria in a *Xylella*-infected Chardonnay vine. D, Intervessel PMs in a *Xylella*-infected U0505-01 vine. Bar in each section equals 5 μm.

to the mAbs in the PMs of PD-resistant grapevine genotypes but were easily detected by the mAbs in the PMs of PD-susceptible grape genotypes. These differences in PM polysaccharide presence or availability could contribute to the differential PD resistance of these grapevine genotypes.

Effects of *X. fastidiosa* Infection on Intervessel PM Integrity in Grapevine Genotypes with Differing PD Resistances and the Intervessel PM Degradation Process in PD-Susceptible Genotypes

Three grapevine genotypes (Chardonnay, U0505-01, and 89-0908, three vines for each genotype) were examined for the integrity of their intervessel PMs 12 weeks after *X. fastidiosa* inoculation; three other plants of each genotype, which were inoculated with phosphate-buffered saline (PBS), were used as controls. In the control vines of all the genotypes (Fig. 3, A and B), intervessel PMs were intact with no pores detectable using the scanning electron microscope (SEM) at a magnification of 20,000. In the *Xylella*-infected vines of the two PD-resistant genotypes (U0505-01 and 89-0908), intervessel PMs were intact in all internodes examined, including the internode with the inoculation site (Fig. 3D). In infected Chardonnay vines, intervessel PMs were intact in vessels that did not contain *Xylella* cells (Fig. 3C), but partially or completely broken intervessel PMs were observed in most bacteria-containing vessels throughout these plants (Fig. 4). When considered along with the distribution of the bacterial cells in the infected vine (described below), this indicates that the disruption of intervessel PM structure and *X. fastidiosa* spread are positively correlated in inoculated PD-susceptible grapevines.

In Chardonnay vines inoculated with *X. fastidiosa*, broken intervessel PMs were found only in the vessels associated with bacterial cells. What appeared to be different stages of intervessel PM degradation were observed in infected vines with severe external PD symptoms and the analysis of these different stages helped to characterize the degradation process (Fig. 4). The first sign of PM degradation was the appearance of small irregular patches with a rough surface; this roughness was scattered mainly across the central band of the PM (Fig. 4A). These patches may have resulted from the removal of some wall material from the PM surface. The loss of the wall material turned the previously tightly packed PM surface into a porous and loose-appearing structure. As more wall material was removed from the PM, a central band region with a rough surface developed and this roughness eventually spread across the width of the PM (Fig. 4B). Pores of different sizes became distinguishable beneath the roughened surface and most of these were round or oval with a diameter of less than 0.10 μm (Fig. 4C). As PM degradation continued, the rough PM surface expanded toward the PM's periphery (Fig. 4D). The frequency and size of the PM pores increased, but the largest pores (usually less than 0.25 μm in diameter) were restricted mostly to the central band region of the PM. Subsequently, the merging of neighboring pores led to a decrease in the number of pores but an increase in their size (Fig. 4F). The pores became irregular (Fig. 4F), round, or oval in shape (Fig. 4G) mostly with sizes ranging from 0.5 to 1.5 μm, and were present across the PM surface. At this time, the two primary cell walls of each PM appeared to be separated, perhaps because of the dissolution of the middle lamella between them. The increased porosity and the

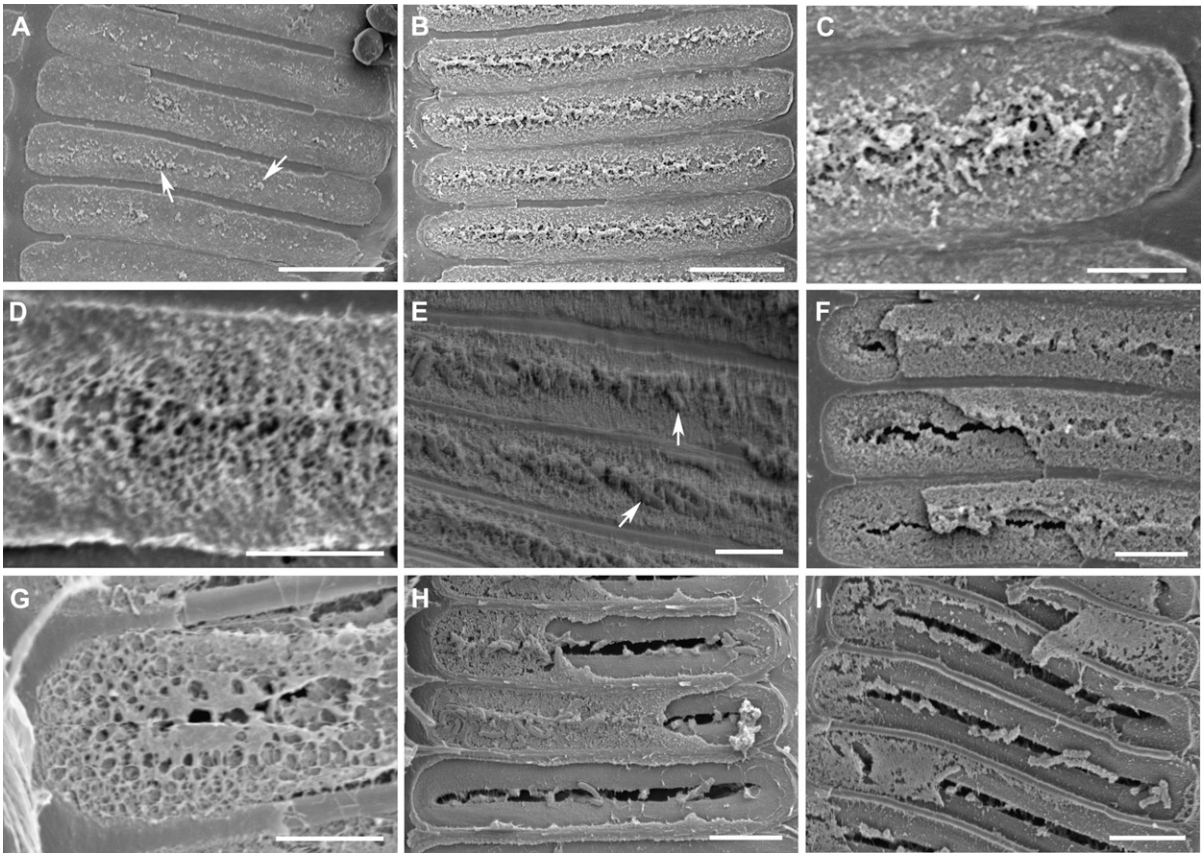

Figure 4. Degradation process of intervessel PMs in PD-susceptible Chardonnay grapevines revealed by SEM. Secondary wall borders of pits were removed to expose the whole PM surface. The progressive stages of PM degradation were shown from A to I except E, which showed the same stage as in D. A, Small patches with a rough surface (arrows) were scattered along the width in the central region of each PM. B, The central band region with a rough surface occurred across the entire PM width. C, An enlarged image of B, showing loosening PM surface and a number of tiny pores in the primary cell wall in the central region of a PM. D, The region with a rough surface has now expanded to the peripheral regions of the PM, and more tiny holes have become visible in the PM's primary cell wall. E, Rough degrading intervessel PMs are associated with *Xylella* cells (arrows). F, The two primary cell walls of each PM are distinguishable. The facing primary wall of each PM had a portion lost and what remained shows many pores. The PM's interior surfaces exposed by the lost wall section have several pores and a crack along the PM's central band region. G, An enlarged PM portion, showing a very porous primary cell wall extending for the entire height of the PM. H, *Xylella* cells are accumulated mostly in the central band regions of porous PMs. I, Part or all of a PM has disappeared. Bar equals 10 μm in A and B; 3 μm in C, D, E, and G; and 5 μm in F, H, and I.

dissolution of the middle lamella might contribute to the weakening of the PM's two primary cell walls. The most common consequence of this was the formation of a crack along the central band region of one or both primary walls, probably due to the concentrated presence of larger-sized pores (Fig. 4, F and G). At this stage, pores and/or cracks in the PM were large enough for the free passage of *Xylella* cells. Further loss of wall material from the two primary walls increased their porosity, eventually leading to the partial or complete removal of one or both primary walls from the PM site (Fig. 4, H and I). Water movement through damaged intervessel PMs could also contribute to the final breakdown of a PM. However, the extent to which water movement occurs in these damaged vessels, which also likely contain vascular system-occluding tyloses and gels (Sun et al., 2006, 2008), is not at all clear. At this stage, the PM has completely lost its role as a barrier to the vessel-to-vessel spread of *X. fastidiosa* cells.

The degradation of the two primary cell walls of each PM usually occurred simultaneously, but it may occur at different rates (Fig. 4F). Differences in rates seemed most obvious later in PM degradation, when the two primary cell walls had separated. Similarly, the degradation of neighboring intervessel PMs may also be uncoordinated (Fig. 4H), although more or less coordinated degradation was often seen (Fig. 4, A, B, E, and I). The degradation of intervessel PMs was observed only in the vessels associated with *Xylella* cells, these often seen on the faces of degrading PMs (Fig. 4, E, H, and I). In some cases, however, bacterial

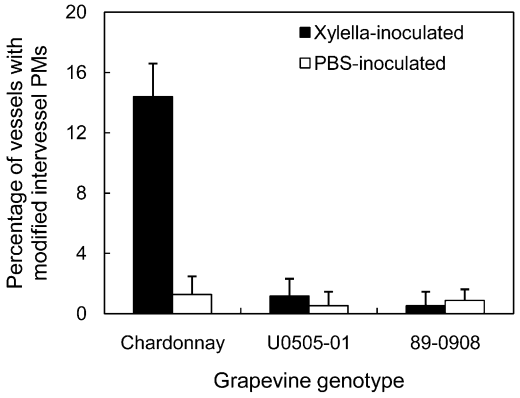

Figure 5. Quantitative comparison of the amounts of vessels with modified intervessel PMs in PD-susceptible (Chardonnay) and -resistant (U0505-01 and 89-0908) genotypes. Each genotype included both *Xylella*-infected vines and PBS-inoculated control vines. Each datum is presented with a mean and SD based on three replicates from three grapevines, respectively. Sixty-three to 88 vessels were observed for each replicate.

cells were observed as many as eight vessel elements away from degrading PMs (Fig. 4, A–D and F). In transverse section vessels with modified intervessel PMs usually formed clusters of multiple cells and appeared to be more or less restricted to a few regions of secondary xylem.

Vessels that were being subjected to degradation were quantitatively compared among the three grapevine genotypes (Fig. 5) and a significant difference was found between the *Xylella*-inoculated PD-susceptible and -resistant lines. The percentage of the vessels with modified intervessel PMs was 14.4% in Chardonnay, but less than 1.2% in U0505-01 and 89-0908. The latter value is not significantly different from that in the corresponding PBS-inoculated controls (Fig. 5). This indicates that even in PD-susceptible grapevines with severe external PD symptoms, only a relatively small portion of the vessels had damaged intervessel PMs.

Distribution of *X. fastidiosa* in Secondary Xylem Tissue of Grapevine Genotypes with Different PD Resistances

This study also investigated distribution of *X. fastidiosa* cells in the 12-week postinoculation vines of the four test grapevine genotypes. In Chardonnay and Riesling vines, bacterial cells were observed in most or all of the internodes examined, including those in the inoculated and noninoculated shoots of each vine (Table I). This indicated not only that the systemic spread of *Xylella* cells occurred in the susceptible vines, but also that the bacterial cells moved downward from the inoculation site on an inoculated shoot, eventually reaching the noninoculated shoot through the common trunk that the two shoots shared. In 89-0908 vines, *Xylella* cells were not observed in the noninoculated shoots of all the vines that were examined. Furthermore, with these PD-resistant vines *Xylella* cells either were not found in the inoculated shoots in vines that were examined or, when pathogen cells were detected, they were seen only within the several internodes downward or upward from the inoculation sites (Table I). A similar situation was seen in the U0505-01 vines examined (Table I). Collectively, these observations demonstrate the localized distribution of *Xylella* cells in the PD-resistant genotypes and their systemic distribution in the PD-susceptible grapevines.

Table I. *Distributional comparison of X. fastidiosa in some exemplary 12-week-postinoculated grapevines with different PD resistances*

The absence or presence of bacterial cells was examined in both inoculated and noninoculated shoots of PD-susceptible grapevine var. Chardonnay (Chardonnay) and grapevine var. Riesling (Riesling) as well as in shoots of PD-resistant *V. arizonica* X *rupestris* (89-0908) and *V. vinifera* X *arizonica* (U0505-01).

Internode[a]	Chardonnay (PD Susceptible)		Riesling (PD Susceptible)		89-0908 (PD Resistant)		U0505-01 (PD Resistant)
	Inoculated Shoot[b]	Noninoculated Shoot	Inoculated Shoot	Noninoculated Shoot	Inoculated Shoot	Noninoculated Shoot	Inoculated Shoot
1	+[c]	+	−	−	−	−	−
3	+	−	+	+	+	−	−
5	+	+	+	−	+	−	+
7	+	+	+	+	−	−	−
9	+	+	−	+	−	−	−
11	+	+	+	+	−	−	−
13	+	+	+	+	−	−	−
15	+	−	+	+	−	−	N/A
17	+	+	+	+	−	N/A	N/A
19	+	+	N/A	+	N/A	N/A	N/A
21	+	N/A[d]	N/A	−	N/A	N/A	N/A
23	+	N/A	N/A	N/A	N/A	N/A	N/A

[a]Internodes are numbered from each shoot base upwards with the first internode at the base as internode 1. [b]Inoculation site was at the sixth internode from the shoot base in all the genotypes except U0505-01 that was inoculated at the fourth internode. [c]+ or − indicates that *Xylella* cells were observed or not observed in a specific internode. [d]N/A represents unavailability of a specific internode due to the short shoot.

DISCUSSION

Intervessel PM Polysaccharide Components Relevant to PD Resistance of Grapevines

Studies of the compositions and structures of polysaccharides isolated from the cell walls of several plant species led to the awareness that cell walls have many features in common (Albersheim, 1976; Carpita and Gibeaut, 1993). A growing awareness of the associations between similar and different polysaccharides in intact cell walls have supported the development of cell wall models that help researchers to understand the relationship between cell wall polysaccharide composition and the stress-bearing abilities of cell walls. This, in turn, supports hypotheses that guide studies aimed at understanding the relationship between specific aspects of cell wall metabolism and plant development (Carpita and Gibeaut, 1993; Albersheim et al., 2010).

Furthermore, use of mAbs that recognize specific wall polysaccharide epitopes (Knox et al., 1990; Knox, 1997; Willats et al., 2000, 2001; Le Goff et al., 2001; Pattathil et al., 2010) has made clear that different cell types in a given tissue can have differing wall compositions. This, in turn, indicates that studies of cell wall metabolism in localized developmental events must consider the relevant heterogeneity in wall structure. Our data for HG and XyG distributions in the PMs of different grapevine genotypes make this point in a potentially useful way. A superficial examination of the data might suggest that intervessel PMs of PD-resistant grapevine genotypes lack weakly ME-HGs and fucosylated XyG. However, our data may indicate merely that the epitopes recognized by JIM5 and CCRC-M1 are not present on the surfaces of the PMs that face the vessel lumens. Our approach for examining PMs is based on cut-open vessels and/or vessels with both ends cut off; in these, interior vessel surfaces including the faces of intervessel PMs are exposed to the primary and secondary mAbs. Our earlier work (Pérez-Donoso et al., 2010), indicating that the average pore in a Chardonnay grapevine PM is approximately 5 to 20 nm in diameter, was based on the ability of proteins of differing shapes and molecular weights to pass through PMs when the proteins were flushed into stem explants. Because of their sizes, it is likely that JIM5 and the other primary mAbs used in our studies would have been excluded from the interiors of the intervessel PMs and we did not attempt to visualize HG and XyG distributions in sections through the thickness of grapevine PMs. In any case, the data presented here indicate, at the minimum, that the organization of PM polysaccharides in the PD-susceptible Chardonnay and Riesling grape varieties differs from that in the PD-resistant *Vitis arizonica* X *rupestris* (89-0908) and *V. vinifera* X *arizonica* (U0505-01) examined here.

Roper et al. (2007) cloned the single putative PG-encoding gene (*pglA*) in the *X. fastidiosa* genome, expressed the sequence in *Escherichia coli*, and showed that the encoded protein digested polygalacturonic acid, an HG pectin. Although it was not tested for the recombinant *Xylella* PG, PGs generally do not digest HG backbones if the polymer has a high degree of methyl esterification. The *X. fastidiosa* genome has three open reading frames whose sequences suggest that they encode EGase-type enzymes (Simpson et al., 2000). One of these putative EGase sequences (*engxcA*) was cloned and expressed in *E. coli*; the encoded protein digested carboxymethyl cellulose and the XyG from tamarind (*Tamarindus indica*) seeds (Pérez-Donoso et al., 2010). When PG and EGase were introduced together into the xylem system of explanted grapevine stems, the enzymes opened holes in the PM surfaces and facilitated the passage of *X. fastidiosa* cells that had been introduced into the explants under pressure. When introduced into explants singly, neither the PG nor the EGase damaged PMs or supported *X. fastidiosa* cell passage through explants (Pérez-Donoso et al., 2010). These observations support the hypothesis that the *Xylella* PG and EGase, together, contribute to PD development by opening the PM barriers and permitting systemic spread of the bacterial population. In fact, Roper et al. (2007) used homologous recombination to inactivate *pglA*, thus creating a PG-minus strain of *X. fastidiosa* and showed that the strain could survive in grapevine shoots into which it had been introduced, but that it did not spread from the point of inoculation or promote the development of PD symptoms. These observations supported the conclusion that *X. fastidiosa*'s PG was a PD virulence factor, at least in the Chardonnay grapes used in this test. Because there were three *Xylella* EGase genes, analogous tests of a possible virulence factor role for EGase in PD development were not attempted.

If the concerted action of *X. fastidiosa*'s PG and EGase is required for the bacterium to move into neighboring vessels from the vessels into which an insect vector has introduced it, then the differences in PM polysaccharides suggested by our immunohistochemical study could help explain the relative PD susceptibilities of the grapevine genotypes examined. Early work examining the abilities of PG and EGase to digest cell wall targets in isolated cell walls indicated that a prior treatment of isolated *Acer pseudoplatanus* walls with PG was needed to maximize the ability of EGase to digest its XyG substrate (Bauer et al., 1973; Keegstra et al., 1973) and the ability of PG to digest a HG pectin backbone is limited by extensive methyl esterification. The fact that the intervessel PMs of the PD-susceptible grape genotypes we tested have a relatively high content of HGs with a relatively low level of esterification suggests that PG action would eventually expose the PM's XyG to EGase action. In contrast, the HG of the intervessel PMs of the resistant 89-0908 and U0505-01 grape germplasm has a relatively high content of methyl esterification (interaction with JIM7, but not JIM5), suggesting that *X. fastidiosa*'s PG would not contribute extensively as a virulence

factor, at least in these PD-resistant lines. Thus, the pathogen's EGase would have reduced access to its XyG target, whether this hemicellulosic substrate is present in these PMs or, as suggested by the CCRC-M1 data, not.

We do not know for certain that the scenario provided here explains the PD resistance shown by the 89-0908 and U0505-01 germplasm. Additional support might be obtained by extending our immunohistochemical survey of intervessel PM polysaccharides to additional grape germplasm. Of course, grapevine resistance to PD might result from a number of factors, not just the limitation of *X. fastidiosa*'s systemic spread suggested by the differences in PM polysaccharide composition/distribution suggested here. Given the importance of PM function in processes other than limitation of pathogen spread, e.g. providing check points that limit vessel embolisms (Sperry et al., 1991, 2005; Choat et al., 2003) and providing pathways for water to move around damaged vessels (Zwieniecki et al., 2001; Tyree and Zimmermann, 2002; Sun et al., 2006, 2008) our adaptation of the use of mAbs to characterize PM polysaccharide compositions may prove useful in explaining other aspects of xylem system function.

Clarification of Intervessel PM Degradation Process

Systemic spread of *X. fastidiosa* cells has been confirmed in grapevines with severe external disease symptoms (Hopkins, 1989) and it has been believed that this spread is achieved through the consecutive vessel-to-vessel movement of the pathogen after intervessel PMs barriers are opened up (Newman et al., 2003; Ellis et al., 2010) due to the action of pathogen CWDEs (Fry and Milholland, 1990a; Purcell and Hopkins, 1996). Lindow and colleagues (Chatterjee et al., 2008; Lindow, 2009) have characterized a diffusible signal factor (DSF) produced by *X. fastidiosa* and the bacterium's DSF response system. They have used reverse transcription real-time PCR to demonstrate that DSF acts to suppress the expression of the pathogen's *pglA* and *engxcA*. *X. fastidiosa* mutants that are unable to produce DSF are hypervirulent on grape (Chatterjee et al., 2008), an observation that supports the importance of CWDEs in systemic *X. fastidiosa* spread. Thus, in grapevine, there appears to be tight regulation of CWDE expression. Several attempts to detect PG and EGase activities when *X. fastidiosa* was grown in the complex periwinkle wilt GelRite culture medium, including periwinkle wilt GelRite medium supplemented with xylem fluid flushed from infected vines using a pressure bomb or supplied with grape cell walls, were unsuccessful (Roper, 2006). More recently, however, Killiny and Almeida (2009) cultured the pathogen in a more simple, defined *X. fastidiosa* medium and used reverse transcription-quantitative PCR to demonstrate relatively low levels of PG and EGase gene expression. In addition, when cultures in *X. fastidiosa* medium were supplemented with pectin or β-glucan from oat (not XyG), the expression of several *X. fastidiosa* genes, including *pglA* and *engxcA*, was up-regulated. Together these results imply that the in planta expression of *X. fastidiosa*'s PG and EGase is controlled by endogenous factors present in the vessel system that are actively modified as the bacterium spreads through the host's xylem.

Direct evidence of bacteria-associated PM dissolution and the details of how *X. fastidiosa*'s enzymatic activities increase the porosity of intervessel PMs to permit the passage of bacterial cells have been lacking. Furthermore, the suggestion of the opening up of the intervessel PMs made previously is based on two reports. The first is the observation of *Xylella* cells on both sides of some intervessel PMs, as viewed under the CLSM (Newman et al., 2003); however, this approach does not reveal details of PM structure. The second comes from the observation of some discontinuities of intervessel PMs viewed using the transmission electron microscope with transverse sections (Ellis et al., 2010). These examinations do not provide direct information on the integrity of an entire intervessel PM. Similarly, no studies describing the intervessel PM degradation process have been reported for other vascular diseases, in which systemic pathogen spread is also crucial for disease symptom development.

Details of the intervessel PM degradation process in infected vines have been clarified in our study (Fig. 4). Most commonly, the degradation started from the narrow central band region in a PM with some tiny pores developing at the outset. This may be because the central band of PM surface polysaccharides is most accessible to the CWDEs, since they must pass through the pit aperture surrounded by the overarching secondary wall to contact the PM surface. Factors such as tensions in the PM wall fabric or chemical differences in these more exposed polymers could also make these polysaccharides better substrates for PG or EGase. The subsequent expansion of the rough surface toward the PM's peripheral region indicated that as the wall materials were gradually removed, sizes of the pores in the PM increased step by step. This allows easier diffusion of pathogen enzymes deeper into and throughout the PM meshwork. The number of pores first increased and later decreased as the pores were enlarged when neighboring pores merged. Eventually, the intervessel PMs may have pores large enough to allow the passage of *X. fastidiosa* cells (Fig. 4, G–I). As described above, weakly ME-HGs and fucosylated XyGs are likely to be included in the wall materials removed from the PMs as their degradation proceeds.

An interesting feature of the degrading process is that the initial removal of wall material leads to loosening of the PM surface; this loose-appearing surface then became increasingly obvious as more and more wall material was removed from the PM. When a PM is intact, as it appears in a healthy vine, its porosity may not allow an efficient approach of the bacterial CWDEs to their substrates that may be masked by other wall components and/or embedded just beneath

the surface of the PM. The formation of an initial loose surface should help create room for the enzymes to access their polysaccharide substrates. The subsequent increase in the area of disintegration of the PM surface should certainly accelerate PM degradation by exposing more polysaccharide targets previously masked. Therefore, when these morphological changes in the PM surface are considered in conjunction with the hydrolytic activity of the bacterial CWDEs, this feature actually reflects the constantly increasing effectiveness of CWDE activity during the PM degrading process and the eventual systemic spread of *X. fastidiosa* in a host plant.

Adjacent PMs may differ to some extent in the rate of degradation although the degradation usually occurred simultaneously in neighboring PMs. This may be explained by spatial differences in CDWE concentrations in different vessels and/or slight differences in polysaccharide richness, including the spatial distributions of polysaccharides relatively close to the PM surfaces that might not be revealed by our current immunohistochemical technique.

This study has also indicated that degrading PMs were observed in the vessels with *X. fastidiosa* cells in the infected PD-susceptible vines, but broken PMs were not always associated with the bacteria cells. Instead, the bacterial cells may be some distances away from the broken PMs. This suggests that the bacterial CWDEs move freely within a vessel and *X. fastidiosa* cells are not required for the localized activities of the enzymes. On the other hand, modified PMs were not observed in the vessels that were not associated with *X. fastidiosa* cells in infected PD-susceptible vines, including the vessels adjacent to those with bacterial cells. This is probably either because the bacterial CWDEs are too large to freely pass through unmodified PM pores as indicated in our earlier report (Pérez-Donoso et al., 2010) or because the CWDEs do not reach sufficiently high concentrations in a vessel without *X. fastidiosa* cells to be effective in polysaccharide digestion. Further investigations on this point are still needed.

MATERIALS AND METHODS

Genotypes and Inoculation of Experimental Grapevines

This investigation dealt with four *Vitis* genotypes: two PD-susceptible genotypes—grapevine (*Vitis vinifera* var. Chardonnay and var. Riesling) and two PD-resistant genotypes—*Vitis arizonica* X *rupestris* (89-0908) and *V. vinifera* X *arizonica* (U0505-01). The growth and treatment for each genotype's vines was carried out as follows. Each grapevine was grown from a grafted root stock in a 7.6-L pot in a greenhouse with a daily 16-h light/8-h dark cycle. Buds of each scion were removed with only two robust buds left at the base and these were then allowed to develop into two shoots. When the vines were 4 weeks old, some were inoculated with *Xylella fastidiosa* as treatment, the others with 0.01 M PBS (0.138 M NaCl, 0.0027 M KCl, pH 7.4) as experimental controls. The *X. fastidiosa* inoculation was carried out only at one shoot of each treated vine at the sixth internode (the fourth or fifth internode in few vines in which the sixth internode was short or had some surface damage) counting from the shoot base. To introduce *X. fastidiosa* into the xylem system of a vine, 60 μL of liquid bacterium inoculum (10^8 colony-forming units mL^{-1}) was transferred with a micropipette to the internode surface and a sterile syringe needle was then used to pierce through the inoculum drop into the xylem. The inoculum was sucked into the xylem when the needle was removed, due to the tension of the transpiration flow in the vine. PBS inoculation for each control vine was done in the same way except that the PBS instead of the *X. fastidiosa* inoculum was used. The two shoots of each control or *X. fastidiosa*-inoculated vine were maintained at 20 to 25 internodes in length by pruning the tops off.

Sample collection started from the fourth week after the inoculation and continued every other week until the 12th week, when most of the inoculated susceptible vines had developed severe external PD symptoms. For each grape genotype, three treated vines and three control vines were used for each sample collection. Three approximately 1-cm-long samples were obtained from each internode of both shoots of each vine. One sample was fixed in formalin-acetic acid-alcohol (Ruzin, 1999) for over 48 h and further used for SEM. The other two were fixed for over 24 h in 4% paraformaldehyde in PEM (50 mM PIPES, 5 mM EGTA, 5 mM $MgSO_4$, pH 6.9; Willats et al., 2002) buffer for further analysis of PM polysaccharide compositions (to be described below).

Conventional SEM to Study Intervessel Pits and PMs

Conventional SEM was employed to study (1) structures of intervessel pits and PMs, (2) integrity of intervessel PMs in both control and *X. fastidiosa*-inoculated vines, and (3) *X. fastidiosa*'s distribution in the secondary xylem of both control and *X. fastidiosa*-inoculated vines of each genotype. Details of the SEM method were described in Sun et al. (2006, 2008) and a brief description is provided here. Small samples were cut from each formalin-acetic acid-alcohol-prefixed internode length, including 2- to 3-mm-thick stem discs exposing the transverse xylem surface and 2- to 3-mm-thick longitudinal segments exposing the radial or tangential xylem surfaces. Trimmed samples were dehydrated via an ethanol series (50%, 60%, 70%, 80%, 90%, 95%, and 100% [twice]) with a 30-min hold at each step. The dehydrated samples were critical-point-dried, gold-palladium-coated, and finally observed under an SEM (Hitachi S3400) at an accelerating voltage of 3 kV (8 kV for some specimens).

Immunohistochemical Technique and CLSM to Detect Polysaccharide Compositions of PMs between Vessels

This study combined an immunohistochemical technique with CLSM (and/or fluorescence microscopy) to identify and compare certain pectic and hemicellulosic polysaccharides in intervessel PMs of the grape genotypes mentioned above. Three monoclonal cell wall antibodies, JIM5, JIM7, and CCRC-M1, were used to recognize HGs and XyGs in the intervessel PMs of healthy vines. The first two rat-derived antibodies can recognize weakly ME-HGs (Vandenbosch et al., 1989; Willats et al., 2000) and heavily ME-HGs (Knox et al., 1990; Willats et al., 2000), respectively, and were obtained from PlantProbes (University of Leeds). The mouse-derived CCRC-M1 recognizes fucosylated XyG (Puhlmann et al., 1994) and was purchased from CarboSource Services at the University of Georgia (Development of CCRC-M1 was supported in part by NSF-RCN grant no. 0090281). Secondary antibodies against CCRC-M1 and the other two wall antibodies were FITC-conjugated goat antimouse IgG (whole molecule; batch no. 057K6068, Sigma-Aldrich) and FITC-conjugated rabbit antirat IgG (whole molecule; batch no. 078K4833, Sigma-Aldrich), respectively.

The protocol using JIM5, JIM7, and CCRC-M1 was modified from Willats et al. (2002). In preparing samples for the immunohistochemical technique with the three primary antibodies, about 1.5-mm-thick xylem segments, exposing the transverse, radial longitudinal, or tangential longitudinal surfaces were trimmed out of the internode samples fixed in 4% paraformaldehyde in PEM buffer. The trimming of samples was conducted in 50 mM PIPES buffer without exposure to air during this period and hereafter. Trimmed sections were washed in PIPES buffer for 45 min followed by incubation in 3% nonfat milk powder in PBS [MP/PBS], pH 7.4 for 1 h to block the antibodies' nonspecific binding sites in the specimens. The samples of each genotype were then divided into four groups: one for incubation with a monoclonal cell wall antibody (primary antibody) and a corresponding FITC-conjugated secondary antibody and the other three for three types of experimental controls to be described below.

The procedure for the incubations of each of the three primary antibodies included submerging sections in a primary antibody diluted in 3% MP/PBS and keeping them at 4°C overnight, washing the sections in PBS three times, 10 min each, and incubating the sections in a corresponding FITC-conjugated

secondary antibody diluted in 3% MP/PBS at room temperature for 1 h. The details regarding the kinds and concentrations of primary and secondary antibodies are described below. The postincubation sections were washed in PBS twice (10 min each) and mounted with antiphotobleaching medium (100 mM Tris, pH 9.2, 50% glycerol, and 1 mg mL^{-1} *p*-phenylenediamine). The sections were then observed and photographed under a CLSM (Leica or Nikon) by using the excitation wavelength of 488 nm and detecting the emission wavelength of 520 ± 2 nm. Some series of images along the *Z* axis (different depths) of a specimen were also taken at 1- or 2-μm intervals, when appropriate, and were accordingly constructed into three-dimensional images.

For each primary antibody, three types of control experiments were set up following the procedure described above, but with the step(s) for the application of primary and/or secondary antibodies omitted. Sections were incubated in (1) 3% MP/PBS only instead of a primary antibody at the step of the application of a primary antibody (control type 1), in (2) 3% MP/PBS instead of a secondary antibody at the step of the application of secondary antibody (control type 2), and in (3) 3% MP/PBS only at both antibody application steps (control type 3).

To get the strongest signal derived from the antibodies and to reduce background noise to a minimal level, trials with the combinations of different concentrations of a primary antibody and the corresponding secondary antibody were first conducted with the PD-susceptible grapevine var. Chardonnay. The original hybridoma supernatant and 3-, 10-, 30-, 100-, 300-, and 1,000-fold dilutions of the hybridoma supernatant in 3% MP/PBS were tested for each of the primary antibodies. The tested concentrations of each of the two secondary antibodies included 25-, 50-, 100-, 200-, 400-, 800-, and 1,600-fold dilutions in 5% MP/PBS. The effectiveness of these antibody concentration combinations was evaluated with a CLSM and/or a fluorescence microscope to define the optimal concentration/concentration range for each antibody. The optimal concentrations/concentration ranges were used for the other grapevine genotypes in this study to detect specific polysaccharide compositions in their intervessel PMs.

ACKNOWLEDGMENTS

We thank Kevin Juzenas and Daisong Kim at the University of Wisconsin-Stevens Point (UWSP) for assistance in SEM observations, Andrew Walker at the University of California-Davis (UCD), and Hong Lin at the U.S. Department of Agriculture-Agriculture Research Services San Joaquin Valley Agricultural Sciences Center (USDA-ARS SJVASC) for providing some PD-resistant grapevine genotypes; Sol Sepsenwol at UWSP for technical support in our usage of SEM, Holly Shugart and Elaine Backus at USDA-ARS SJVASC, and James Lincoln and David Gilchrist at UCD for making it possible for us to use the CLSMs in their facilities; Carlos Crisosto at UCD for coordinating Sun's research trips in California, and Caroline Roper at UC-Riverside and James Lincoln at UCD for the *X. fastidiosa* inoculum. Some Chardonnay vines in this study were obtained from Duarte Nursery, Inc., Hughson, CA.

Received November 2, 2010; accepted February 19, 2011; published February 22, 2011.

LITERATURE CITED

Albersheim P (1976) The primary cell wall. *In* J Bonner, JE Varner, eds, Plant Biochemistry, Ed 3. Academic Press, New York, pp 225–274

Albersheim P, Darvill A, Roberts K, Sederoff R, Staehelin A (2010) Plant Cell Walls (From Chemistry to Biology). Garland Science, New York, pp 43–66

Barras F, Van Gijsegem F, Chatterjee AK (1994) Extracellular enzymes and pathogenesis of soft-rot *Erwinia.* Annu Rev Phytopathol **32:** 201–234

Bauer WD, Talmadge KW, Keegstra K, Albersheim P (1973) The structure of plant cell walls. II. The hemicellulose of the walls of suspension-cultured sycamore cells. Plant Physiol **51:** 174–187

Carpita NC, Gibeaut DM (1993) Structural models of primary cell walls in flowering plants: consistency of molecular structure with the physical properties of the walls during growth. Plant J **3:** 1–30

Chatelet DS, Matthews MA, Rost TL (2006) Xylem structure and connectivity in grapevine (*Vitis vinifera*) shoots provides a passive mechanism for the spread of bacteria in grape plants. Ann Bot (Lond) **98:** 483–494

Chatterjee S, Wistrom C, Lindow SE (2008) A cell-cell signaling sensor is required for virulence and insect transmission of *Xylella fastidiosa.* Proc Natl Acad Sci USA **105:** 2670–2675

Choat B, Ball M, Luly J, Holtum J (2003) Pit membrane porosity and water stress-induced cavitation in four co-existing dry rainforest tree species. Plant Physiol **131:** 41–48

Ellis EA, McEachern RM, Clark S, Cobb BG (2010) Ultrastructure of pit membrane dissolution and movement of *Xylella fastidiosa* through pit membranes in petioles of *Vitis vinifera.* Botany **88:** 596–600

Esau K (1977) Anatomy of Seed Plants, Ed 2. John Wiley and Sons, Inc., New York, pp 43–60

Evert RF (2006) Esau's Plant Anatomy, Ed 3. John Wiley and Sons, Inc., Hoboken, New Jersey, pp 91–102

Fleischer A, O'Neill MA, Ehwald R (1999) The pore size of non-graminaceous plant cell walls is rapidly decreased by borate ester cross-linking of the pectic polysaccharide rhamnogalacturonan II. Plant Physiol **121:** 829–838

Fry SM, Milholland RD (1990a) Multiplication and translocation of *Xylella fastidiosa* in petioles and stems of grapevine resistant, tolerant and susceptible to Pierce's disease. Phytopathology **80:** 61–65

Fry SM, Milholland RD (1990b) Response of resistant, tolerant and susceptible grapevine tissues to invasion by the Pierce's disease bacterium, *Xylella fastidiosa.* Phytopathology **80:** 66–69

Hopkins DL (1989) *Xylella fastidiosa*: xylem-limited bacterial pathogen of plants. Annu Rev Phytopathol **27:** 271–290

Hopkins DL, Mollenhauer HH (1975) Tylose and gum formation in the xylem of Pierce's disease infected grapevines. Proc Amer Phytopathol Soc **2:** 65

Keegstra K, Talmadge KW, Bauer WD, Albersheim P (1973) The structure of plant cell walls. III. A model of the cell walls of suspension-cultured sycamore cells based on the interconnections of the macromolecular components. Plant Physiol **51:** 188–197

Killiny N, Almeida RPP (2009) Host structural carbohydrate induces vector transmission of a bacterial plant pathogen. Proc Natl Acad Sci USA **106:** 22416–22420

Knox JP (1997) The use of antibodies to study the architecture and developmental regulation of plant cell walls. Int Rev Cytol **171:** 79–120

Knox JP, Linstead PJ, King J, Cooper C, Roberts K (1990) Pectin esterification is spatially regulated both within cell walls and between developing tissues of root apices. Planta **181:** 512–521

Krivanek AF, Walker MA (2005) *Vitis* resistance to Pierce's disease is characterized by differential *Xylella* populations in stems and leaves. Phytopathology **95:** 44–52

Le Goff A, Renard CMGC, Bonnin E, Thibault J-F (2001) Extraction, purification and chemical characterization of xylogalacturonans from pea hulls. Carbohydr Polym **45:** 325–334

Lindow SE (2009) Control of Pierce's disease by method involving pathogen confusion. Proceedings of the 2009 Pierces Disease Research Symposium, California Department of Food and Agriculture, pp 150–157

Loomis NH (1958) Performance of *Vitis* species in the south as an indication of their relative resistance to Pierce's disease. Plant Dis Rep **42:** 833–836

Mollenhauer HH, Hopkins DL (1974) Ultrastructural study of Pierce's disease bacterium in grape xylem tissue. J Bacteriol **119:** 612–618

Newman KL, Almeida RPP, Purcell AH, Lindow SE (2003) Use of a green fluorescent strain for analysis of *Xylella fastidiosa* colonization of *Vitis vinifera.* Appl Environ Microbiol **69:** 7319–7327

Newman KL, Almeida RPP, Purcell AH, Lindow SE (2004) Cell-cell signaling controls *Xylella fastidiosa* interactions with both insects and plants. Proc Natl Acad Sci USA **101:** 1737–1742

Pattathil S, Avci U, Baldwin D, Swennes AG, McGill JA, Popper Z, Bootten T, Albert A, Davis RH, Chennareddy C, et al (2010) A comprehensive toolkit of plant cell wall glycan-directed monoclonal antibodies. Plant Physiol **153:** 514–525

Pérez-Donoso AG, Sun Q, Roper MC, Greve LC, Kirkpatrick B, Labavitch JM (2010) Cell wall-degrading enzymes enlarge the pore size of intervessel pit membranes in healthy and *Xylella fastidiosa*-infected grapevines. Plant Physiol **152:** 1748–1759

Puhlmann J, Bucheli E, Swain MJ, Dunning N, Albersheim P, Darvill AG, Hahn MG (1994) Generation of monoclonal antibodies against plant cell-wall polysaccharides. I. Characterization of a monoclonal antibody to a terminal α-(1→2)-linked fucosyl-containing epitope. Plant Physiol **104:** 699–710

Purcell AH, Hopkins DL (1996) Fastidious xylem-limited bacterial plant pathogens. Annu Rev Phytopathol **34:** 131–151

Roper MC (2006) The characterization and role of *Xylella fastidiosa* plant cell wall degrading enzymes and exopolysaccharide in Pierce's disease of grapevine. PhD dissertation. University of California, Davis, CA

Roper MC, Greve LC, Warren JG, Labavitch JM, Kirkpatrick BC (2007) *Xylella fastidiosa* requires polygalacturonase for colonization and pathogenicity in *Vitis vinifera* grapevines. Mol Plant Microbe Interact **20:** 411–419

Ruel JJ, Walker MA (2006) Resistance to Pierce's disease in *Muscadinia rotundifolia* and other native grape species. Am J Enol Vitic **57:** 158–165

Ruzin SE (1999) Plant Microtechnique and Microscopy. Oxford University Press, New York, pp 33–56

Simpson AJG, Reinach FC, Arruda P, Abreu FA, Acencio M, Alvarenga R, Alves LM, Araya JE, Baia GS, Baptista CS, et al (2000) The genome sequence of the plant pathogen *Xylella fastidiosa*. Nature **406:** 151–159

Sperry JS, Hacke UG, Wheeler JK (2005) Comparative analysis of end wall resistivity in xylem conduits. Plant Cell Environ **28:** 456–465

Sperry JS, Perry AH, Sullivan JEM (1991) Pit membrane degradation and air-embolism formation in ageing xylem vessels of *Populus tremuloides* Michx. J Exp Bot **42:** 1399–1406

Sun Q, Rost TL, Matthews MA (2006) Pruning-induced tylose development in stems of current-year shoots of *Vitis vinifera* (Vitaceae). Am J Bot **93:** 1567–1576

Sun Q, Rost TL, Matthews MA (2008) Wound-induced vascular occlusions in *Vitis vinifera* (Vitaceae): tyloses in summer and gels in winter. Am J Bot **95:** 1498–1505

Sun Q, Rost TL, Reid MS, Matthews MA (2007) Ethylene and not embolism is required for wound-induced tylose development in stems of grapevines. Plant Physiol **145:** 1629–1636

Tattar TA (1989) Diseases of Shade Trees, Revised Ed. Academic Press, New York, pp 18–33

Thorne ET, Young BM, Young GM, Stevenson JF, Labavitch JM, Matthews MA, Rost TL (2006) The structure of xylem vessels in grapevine and a possible passive mechanism for the systemic spread of bacterial disease. Am J Bot **93:** 497–504

Tyree MT, Zimmermann MH (2002) Xylem Structure and the Ascent of Sap, Ed 2. Springer-Verlag, Berlin, pp 89–142

Vandenbosch KA, Bradley DJ, Knox JP, Perotto S, Butcher GW, Brewin NJ (1989) Common components of the infection thread matrix and the intercellular space identified by immunocytochemical analysis of pea nodules and uninfected roots. EMBO J **8:** 335–341

Varela LG, Smith RJ, Phillips PA (2001) Pierce's Disease. Publication 21600. University of California, Division of Agricultural and Natural Resources, Oakland, CA, pp 10–14

Willats WGT, Orfila C, Limberg G, Buchholt HC, van Alebeek GJWM, Voragen AGJ, Marcus SE, Christensen TMIE, Mikkelsen JD, Murray BS, et al (2001) Modulation of the degree and pattern of methyl-esterification of pectic homogalacturonan in plant cell walls: implications for pectin methyl esterase action, matrix properties, and cell adhesion. J Biol Chem **276:** 19404–19413

Willats WGT, Steele-King CG, Marcus SF, Knox JP (2002) Antibody techniques. *In* PM Gilmartin, C Bowler, eds, Molecular Plant Biology, Vol 2, A Practical Approach. Oxford University Press, Oxford, pp 199–220

Willats WGT, Steele-King CG, McCartney L, Orfila C, Marcus SE, Knox JP (2000) Making and using antibody probes to study plant cell walls. Plant Physiol Biochem **38:** 27–36

Zwieniecki MA, Melcher PJ, Michele Holbrook NM (2001) Hydrogel control of xylem hydraulic resistance in plants. Science **291:** 1059–1062